

Extended Benders Decomposition for CVaR-constrained unit commitment decisions in pan-European energy system models considering feed-in uncertainties

Moritz Nobis, Alexander Lindner, Carlo Schmitt

Institute for High Voltage Technology

RWTH Aachen University

Aachen, Germany

moritz.nobis@rwth-aachen.de

Abstract

The energy system decarbonization leads to an increasing relevance of intraday markets to balance forecasting uncertainties from fluctuating renewable energy sources. The evaluation of profit opportunities on the intraday market and the determination of the future demand for flexible power plants by fundamental models is currently limited. Due to computational complexity, fundamental energy system models focus on only two configurations at present. Either technical and economic constraints are modelled in detail, but deterministically, or they are simplified considerably, allowing for uncertainty and partly risk-constrained modelling. In this paper, a novel method enabling the integration of forecasting errors and risk aversion into a pan-European fundamental power plant optimization model is presented to adequately evaluate the business model and the technical market behaviour of power plants in energy systems with a high penetration of renewables. This is realized by nesting of a Lagrangian Relaxation and an extended Benders decomposition. We show that the process converges rapidly and grows only linearly with the number of scenarios considered.

Index Terms

Benders Decomposition, CVaR, Forecasting Errors, Lagrangian Relaxation, Stochastic Unit Commitment

I. INTRODUCTION

Climate policy promote an increasing share of renewable energies in gross final energy consumption, which is set to reach 27% in the EU and 30% in Germany by 2030 [1] [2] [3] [4]. The expansion and use of renewables primarily occurs in the electricity sector, which along with the heating sector, both in Germany and worldwide, accounts for the largest share of total emissions of climate-relevant gases [5] [6].

The focus of the renewables expansion lays on wind energy (WTGS) and photovoltaic (PV) plants, which account for 88% of the total energy output of all renewables installed by the end of 2017 in Germany [5]. Due to their

supply-dependent and thus hard to predict feed-in characteristics, marketers of WTGS and PV (so-called direct marketers) are exposed to a significant volume risk in contrast to conventional generation plants [7]. In addition to the uncertainty of supply-dependent generation, the electrical system load also exhibits stochastic behaviour in some cases. With the introduction of the intraday market (ID) in 2007, a marketing platform was created for compensating forecasting errors distorting the DA market (DA). The absolute forecasting errors and thus the trading volume and liquidity on the ID market have grown steadily in proportion to the addition of fluctuating renewables in recent years [5] [8].

After using dispatch optimization and load management in a portfolio, the remaining forecasting errors are compensated by a counterparty on the ID market. This can either be the operator of a storage power plant or of flexible conventional power plants [9]. The market counterparty - balancing the forecasting errors - should thereby have retained the necessary flexibility at upstream market levels, such as the DA market. The market participant must therefore already consider the possible sales on the ID market during the marketing decision on the DA market. Due to the stochastic character of the trading volumes and prices, however, the return is unknown *ex ante* and can therefore only be approximated using methods of uncertainty quantification. By participating in the ID market, the operators of flexible assets are offered opportunities exposed to a price risk [7]. Participation in the ID market is optional for flexibilities; for direct marketers, however, participation is mandatory due to the obligation to adhere to their balancing groups supply and consumption equilibrium [10].

The evaluation of technology portfolios and regulatory decisions in the energy market during this transformation process requires a model framework that fundamentally reproduces realistic interactions in unit commitment for scenarios of a future energy system. The commitment decisions must reflect the real decision-making process of power plant operators. This implies the consideration of several market stages under uncertainty and risk-averse decision-making. The adequate mapping of technical and economic constraints of individual units thus is as important as the endogenous consideration of market coupling.

The described research questions will be addressed in this paper, which presents a significant distinguishing feature from the state-of-the-art:

- 1) *Methods using perfect foresight decisions:* Current large scale dispatch optimization models considering all inter-connected market zones in the ENTSO-E area usually focus only on decisions under perfect foresight [11] [12] [13] [14]. Some include detailed constraints allowing for unit commitment decisions [15] [16] [17] [18]. Only few approaches take into account simplified multistage decisions [19].
- 2) *Stochastic meta-heuristic approaches:* Heuristic approaches lack the guarantee of optimality and have only been applied to small test systems [20] [21] [22].
- 3) *Stochastic mathematical optimization approaches:* Ensuring the solution's optimality and the process' transparency can only be achieved by applying mathematical optimization methods. Various approaches considering i.i.d. uncertainties [23] [24] [25] [26] and time-dependent uncertainties, modelled either through markov-chains [27] or

time series analysis approaches [28] [29] [30] [31] [32], exist. Scenario reduction methods are partially used to handle solvability issues in high dimensional models [33] [34] [35] [36]. The integration of risk measures associated with the depicted uncertainties leads to a significant increase in complexity and is therefore used in test systems only [24] [25] [36]. So far, there are hardly any approaches that consider complex power plant restrictions requiring integer decision variables. In general linear approximations of these constraints have been realized [33]. In order to economically evaluate the operating decisions of individual plants or to be able to carry them out on a system-wide level, it is necessary for electricity market models to generate market clearing prices. Such market clearing prices must reflect the market participant's decision undistortedly. This implies that unit commitment decisions of all individual plants based on the modelled market prices lead to the same decision as the model endogenous unit commitment decision. This in turn requires a suitable and detailed modelling of specific causal relations and influencing factors such as the adequate representation of start-up costs in the electricity prices [28] [34]. The formulation of the stochastic unit commitment problem as a mathematical optimization model poses great challenges for the available computing resources, so that the market zones depicted in the literature are predominantly limited to test networks or small supply areas [23] [24] [25] [26] [27] [28] [32] [34] [36]. Only publications envisaging the Wilmar Joint Market Model [29] [30] [33] and a second approach [35] depict real-scale systems such as the German or the Irish market areas [31] but without complex restrictions.

This paper presents a procedure enabling the integration of forecasting errors of fluctuating renewable energies and the electrical system load into a pan-European fundamental power plant optimization model taking into account risk averse decision-making. All relevant techno-economic constraints of several thousand single units are considered [37]. The integration of unit commitment decisions based on the Conditional Value-at-Risk (CVaR) ensures a realistic decision process of each unit with regard to the trade off between DA- and/or ID participation. Additionally, all market areas within the European interconnected system including endogenous market coupling are taken into account. Section II presents an overview of the overlaying Lagrangian Relaxation coordinating the bid-ask matching and the market coupling for the pan-European power system. Subsequently, the single power plant optimization is described for thermal and for hydro power plants separately. In section III the decomposition of thermal units is depicted followed by the modelling of hydro power plants in section IV. The advantages of the decomposition over the closed formulation are benchmarked in section V. Section VI provides a complete overview on the convergence behaviour of the nesting Lagrangian Relaxation and extended Benders decomposition. Concluding, the findings and suggestions for future research are presented in section VII.

II. PAN-EUROPEAN POWER PLANT OPTIMIZATION

Fundamental energy system models based on unit commitment approaches in general aim at cost minimization, which converges into real market behaviour in markets with uniform pricing [18]. The joint consideration of the DA and the ID market subject to forecasting uncertainties can be represented by a two-stage linear programming approach [7]. The first stage consists of the objective function $c^T x$ subject to the set of constraints from eq. (2). The second stage consists of the π_ω -weighted objective functions $q_\omega^T y_\omega$ representing a set Ω of discrete scenarios. The latter is restricted by the recourse matrix $W y_\omega$ and the technology matrix \mathcal{T}_ω coupling to the first-stage, which must correspond to the vector h_ω .

$$\min_{x, y_\omega} z = c^T x + \sum_{\omega \in \Omega} \pi_\omega q_\omega^T y_\omega, \quad (1)$$

$$\text{s.t.} \quad Ax = b \quad (2)$$

$$\mathcal{T}_\omega x + W y_\omega = h_\omega \quad (3)$$

$$x \geq 0, \quad y_\omega \geq 0, \quad \sum_{\omega \in \Omega} \pi_\omega = 1, \quad \omega \in \Omega. \quad (4)$$

Applying the concept to an energy system consisting of K units covering C countries for T time steps, where T usually corresponds to an annual simulation in hourly resolution, the following objective function can be formulated

$$\min \underbrace{\sum_{c \in C} \sum_{k \in K_c} \sum_{t \in T} (a_{c,k} \nu_{c,k,t}^{\text{DA}} + \text{suc}_{c,k,t}^{\text{DA}})}_{\text{DA-Costs } K^{\text{DA}}(x_{c,k,t}^{\text{DA}})} + \underbrace{\sum_{c \in C} \sum_{k \in K_c} \sum_{t \in T} \sum_{\omega \in \Omega} \pi_\omega (b_{k,c} P_{c,k,t,\omega}^{\text{Phy}})}_{\text{Expected ID-Costs } \mathbb{E}(K^{\text{ID}}(x_{c,k,t,\omega}^{\text{ID}}))}. \quad (5)$$

The unit commitment decision $\nu_{c,k,t}^{\text{DA}}$ (with $\nu \in \mathbb{B} = \{0, 1\}$) is taken in the first stage eventually causing fixed costs $a_{c,k}$. If the unit changes its commitment state from offline (0) to online (1) start costs $\text{suc}_{c,k,t}^{\text{DA}}$ accrue. The start costs depend on how long the unit was offline before considering the additional expenditure caused by heating up cold boilers and turbines according to [37]. The physical power output $P_{c,k,t,\omega}^{\text{Phy}}$ is determined in the second stage for each probability-weighted scenario considering a linear cost term $b_{k,c}$. The physical power is splitted up to provide power for the DA $P_{c,k,t}^{\text{DA}}$ and ID market $P_{c,k,t}^{\text{ID}}$ (not relevant for the objective function as their coefficients equal zero).

The coupling constraints 6 and 7 ensure that the power output of all endogenously optimized units equal the load $D_{c,t}^{\text{DA/ID}}$ including exogenously defined REN-feed-in $EE_{c,t}^{\text{DA/ID}}$ and market coupling decisions $MC_{c,t}^{\text{DA/ID}}$.

$$D_{c,t}^{\text{DA}} = \sum_{k \in K_c} P_{c,k,t}^{\text{DA}} + EE_{c,t}^{\text{DA}} + MC_{c,t}^{\text{DA}}, \quad c \in C, t \in T \quad (6)$$

$$D_{c,t,\omega}^{\text{ID}} = \sum_{k \in K_c} P_{c,k,t,\omega}^{\text{ID}} + EE_{c,t,\omega}^{\text{ID}} + MC_{c,t,\omega}^{\text{ID}}, \quad c \in C, t \in T, \omega \in \Omega. \quad (7)$$

Langrangian Relaxation is applied to use the advantage of parallel computing. Furthermore, each additionally regarded scenario leads to a quadratic increase of the MIP's size, which represents a key influencing factor for its

solvability and computing time. Therefore, an existing deterministic approach [18] is advanced by integrating it's stochastic extension to

$$\begin{aligned} \max_{\lambda_{c,t}^{\text{DA}}, \lambda_{c,t,\omega}^{\text{ID}}} \left\{ \min \sum_{c \in C} \sum_{k \in K_c} \sum_{t \in T} (a_{c,k} \nu_{c,k,t}^{\text{DA}} + \text{suc}_{c,k,t}^{\text{DA}}) + \sum_{c \in C} \sum_{k \in K_c} \sum_{t \in T} \sum_{\omega \in \Omega} \pi_{\omega} b_{c,t} P_{c,k,t}^{\text{Phy}} \right. \\ \left. - \sum_{c \in C} \sum_{t \in T} \lambda_{c,t}^{\text{DA}} \left(\sum_{k \in K_c} P_{c,k,t}^{\text{DA}} + EE_{c,t}^{\text{DA}} + MC_{c,t}^{\text{DA}} - D_{c,t}^{\text{DA}} \right) \right. \\ \left. - \sum_{c \in C} \sum_{t \in T} \sum_{\omega \in \Omega} \pi_{\omega} \lambda_{c,t,\omega}^{\text{ID}} \left(\sum_{k \in K_c} P_{c,k,t,\omega}^{\text{ID}} + EE_{c,t,\omega}^{\text{ID}} + MC_{c,t,\omega}^{\text{ID}} - D_{c,t,\omega}^{\text{ID}} \right) \right\}. \end{aligned} \quad (8)$$

$\lambda_{c,t}^{\text{DA}}, \lambda_{c,t,\omega}^{\text{ID}} \in \mathbb{R}$: Lagrangian-Multiplier DA/ID

Each single unit's contribution margin can thereby be maximized (corresponds to minimizing the unit's costs) subject to its specific Lagrangian multipliers independently

$$\min \sum_{t \in T} (a_{c,k} \nu_{c,k,t}^{\text{DA}} + \text{suc}_{c,k,t}^{\text{DA}} - \lambda_{c,t}^{\text{DA}} P_{c,k,t}^{\text{DA}}) + \sum_{t \in T} \sum_{\omega \in \Omega} \pi_{\omega} (b_{c,t} P_{c,k,t}^{\text{Phy}} - \lambda_{c,t,\omega}^{\text{ID}} P_{c,k,t,\omega}^{\text{ID}}). \quad (9)$$

The adjustment of the Lagrangian multipliers is performed in an iterative process using a subgradient approach until convergence is reached. Furthermore, the Lagrangian multipliers of a relaxed demand constraint - designated as shadow prices - can be interpreted as uniform market prices [38].

The objective function $F(x)$ according to eq. (9) leads to an optimization of the expected value and thus assumes risk-neutral behavior of the power plant operator. Let $f(x, \omega)$ be the objective value, which results in a specific scenario ω

$$f(x, \omega) = \underbrace{\sum_{t \in T} (a \cdot \nu_t^{\text{DA}} + \text{suc}_t^{\text{DA}} - \lambda_t^{\text{DA}} P_t^{\text{DA}})}_{\text{DA-Part}} + \underbrace{\sum_{t \in T} (b \cdot P_{t,\omega}^{\text{Phy}} - \lambda_{t,\omega}^{\text{ID}} P_{t,\omega}^{\text{ID}})}_{\text{ID-Part}}, \quad (10)$$

then

$$F(x) = \mathbb{E}(f(x, \omega)). \quad (11)$$

In reality, however, power plant operators do not trade as risk-neutral actors, but rather try to avoid potential losses in individual ID scenarios or at least limit them. This risk-averse behaviour can be depicted in the individual power plant optimization by the introduction of a suitable risk measure. This paper suggests and applies the CVaR, a coherent risk measure preserving the convexity of the optimization problem [39]. The CVaR can be interpreted as the conditional mean of the loss distribution above the α -quantile. The CVaR is added to the objective function multiplied by a weighting factor β :

$$F(x) = \mathbb{E}(f(x, \omega)) + \beta \cdot \text{CVaR}_{\alpha}(f(x, \omega)). \quad (12)$$

The value of β determines the impact of the risk measure on the optimization results. The translation invariance of the CVaR allows for the integration of eq. (12) into eq. (9) as follows

$$\begin{aligned} F(x) = (1 + \beta) \sum_{t \in T} (a \cdot \nu_t^{\text{DA}} + \text{suc}_t^{\text{DA}} - \lambda_t^{\text{DA}} P_t^{\text{DA}}) \\ + \sum_{\omega \in \Omega} \sum_{t \in T} \pi_{\omega} (b \cdot P_{t,\omega}^{\text{Phy}} - \lambda_{t,\omega}^{\text{ID}} P_{t,\omega}^{\text{ID}}) + \beta \cdot \text{CVaR}_{\alpha}. \end{aligned} \quad (13)$$

with CVaR_α according to [40]:

$$\text{CVaR}_\alpha = \text{VaR}_\alpha + \frac{1}{1-\alpha} \sum_{\omega \in \Omega} \pi_\omega \eta_\omega \quad (14)$$

$$\eta_\omega \geq \sum_{t \in T} \left(b \cdot P_{t,\omega}^{\text{Phy}} - \lambda_{t,\omega}^{\text{ID}} P_{t,\omega}^{\text{ID}} \right) - \text{VaR}_\alpha, \quad \omega \in \Omega \quad (15)$$

$$\text{VaR}_\alpha \in \mathbb{R}, \eta_\omega \geq 0. \quad (16)$$

III. DECOMPOSITION APPROACH OF THERMAL POWER PLANTS

The power plant models as introduced above are characterized by a block-angular structure of the constraint matrix, which comprises both decision stages. This means that some of the constraints – represented by the matrix A and the right-hand side b – exclusively refer to the first-stage, i.e. DA, variables, whereas other constraints – represented by the matrices T_ω and W and the right-hand side h_ω – have to be satisfied conjointly and are thus coupling the ID decisions per scenario $\omega \in \Omega$ to the DA decisions.

The specific problem structure yields a quadratic growth of the problem size with an increasing number $|\Omega|$ of ID scenarios. Furthermore, the thermal power plant models exhibit a high model complexity at already few scenarios mainly due to the binary unit commitment decision variables. Respective implications for the computing requirements (storing and solving the models) render decomposition approaches indispensable for complexity purposes. The block-angular structure suggests the application of a Benders decomposition, also known as the L-shaped algorithm [41]. Apart from the requirements associated with the specific problem structure, the Benders decomposition requires the second-stage variables to be all continuous, which is fulfilled in our case since the binary decision to determine if a power plant will be online or not is already made in the first-stage. When considering the risk measure CVaR in the decision process of the power plants the classic Benders decomposition framework exhibits a significant disadvantage in the sense that for some model instances the number of required algorithm iterations is inadmissibly high. This can be explained by the fact that in the classic Benders decomposition the second-stage recourse – that means both expected costs and ID CVaR – are estimated by a single class of constraints (see below) and thus cannot adequately reflect the heterogeneity of the two measures for particular model instances. As a consequence the classic Benders decomposition has been adapted and extended according to the findings in [42]. The algorithm and the exact formulation of this new approach for our single unit commitment problem are explained in detail below.

A. General decomposition process

The general process of the extended decomposition algorithm is identical to the one the classic Benders decomposition. As a first step, the extensive formulation as given in section II is split along its block-angular structure into a master problem (MP) and $|\Omega|$ subproblems (SP) for each discrete ID scenario. Hereby, the master problem reflects the decision making process of the first stochastic stage, whereas the subproblems represent the second stochastic stage whose decisions depend on the first-stage decisions on the one hand and on the scenario-specific parameters on the other hand. The general idea of the algorithm is to iteratively determine an optimal solution for the master

problem and pass it on to the subproblems. Based on the fixed first-stage decision variables, we subsequently try to optimally solve the subproblems. Depending on the feasibility of the subproblems for the particular first-stage decision, different classes of cutting planes (optimality cuts or feasibility cuts) are added to the master problem. With each cut the solution space is reduced step by step such that the combination of the first- and second-stage decisions will converge towards the overall optimum. The mathematical description of the master problem for our particular and extended case is given by:

$$\min_{x^{\text{DA}}, \theta^{\mathbb{E}}, \theta^{\text{CVaR}}, VaR_i, \eta_{i,\omega}} (1 + \beta) \sum_{t \in T} (a \cdot \nu_t^{\text{DA}} + \text{suc}_t^{\text{DA}} - \lambda_t^{\text{DA}} P_t^{\text{DA}}) + \theta^{\mathbb{E}} + \beta \cdot \theta^{\text{CVaR}} \quad (17)$$

$$s.t. Ax^{\text{DA}} \leq b \quad (18)$$

$$\theta^{\mathbb{E}} \geq e_i - E_i x^{\text{DA}} \quad i = 1, \dots, \tau \quad (19)$$

$$0 \geq d_j - D_j x^{\text{DA}} \quad j = 1, \dots, \sigma \quad (20)$$

$$x^{\text{DA}} = (\nu^{\text{DA}}, \text{suc}^{\text{DA}}, P^{\text{DA}})^{\text{T}} \quad (21)$$

$$\theta^{\text{CVaR}} \geq VaR_i + \frac{1}{1 - \alpha} \sum_{\omega \in \Omega} \pi_{\omega} \eta_{i,\omega} \quad i = 1, \dots, \tau \quad (22)$$

$$\eta_{i,\omega} \geq \hat{e}_{i,\omega} - \hat{E}_{i,\omega} x^{\text{DA}} - VaR_i \quad i = 1, \dots, \tau, \omega \in \Omega \quad (23)$$

$$\eta_{i,\omega} \geq 0 \quad i = 1, \dots, \tau, \omega \in \Omega \quad (24)$$

$$VaR_i \in \mathbb{R} \quad i = 1, \dots, \tau. \quad (25)$$

Apart from the first-stage decision variables x^{DA} the master problem contains the additional auxiliary variables $\theta^{\mathbb{E}}$ and θ^{CVaR} , which represent an approximation of the expected second-stage recourse cost over all ID scenarios and the resulting second-stage CVaR, respectively. σ and τ denote the number of feasibility cuts (20) and optimality cuts (19) (22) introduced in previous iterations. In opposition to the classic Benders decomposition, the extended method features different classes of optimality cuts for $\theta^{\mathbb{E}}$ and θ^{CVaR} in order to build distinct linear approximations for both the expected recourse and CVaR of the second stage. The CVaR optimality cuts in (22) are supported by the auxiliary constraints (23) - (25). Note that with every optimality cut i we introduce separate copies of the auxiliary variables VaR_i and $\eta_{i,\omega}$. Thus, the extended Benders decomposition constitutes a combined column and row generation procedure. Let $(x^{\text{DA}^\nu}, \theta^{\mathbb{E}^\nu}, \theta^{\text{CVaR}^\nu}, VaR_i^\nu, \eta_{i,\omega}^\nu)^{\text{T}}$ be the optimal solution to the master problem for Benders iteration ν . The fixed optimal value for x^{DA^ν} is passed on to the subproblems, which are then solved to find an optimal decision for their respective ID scenario $\omega \in \Omega$ depending on the given DA decision and the scenario specific parameters. The subproblems are given by

$$Q(x^{\text{DA}^\nu}, \omega) = \min_{x_{t,\omega}^{\text{ID}}} \sum_{t \in T} (b \cdot P_{t,\omega}^{\text{ID}} - \lambda_{t,\omega}^{\text{ID}} P_{t,\omega}^{\text{Phy}}) \quad (26)$$

$$s.t. W x_{\omega}^{\text{ID}} \leq h_{\omega} - T_{\omega} x^{\text{DA}^\nu} \quad (27)$$

$$x_{\omega}^{\text{ID}} = (P_{t,\omega}^{\text{ID}}, P_{t,\omega}^{\text{Phy}})^{\text{T}}. \quad (28)$$

When solving the subproblems, two cases can occur:

1) *All subproblems $\omega \in \Omega$ can be solved to optimality:* If the stopping condition of the algorithm (see below) is not yet fulfilled, the solutions of the subproblems may be optimal for the given first-stage decision x^{DA^ν} , but the combined solution $\left(x^{\text{DA}^\nu}, x_{\omega=1}^{\text{ID}^\nu}, \dots, x_{\omega=|\Omega|}^{\text{ID}^\nu}\right)^\text{T}$ is not yet optimal for the overall problem. In order to receive a better combined solution in the next iteration $\nu + 1$ we introduce distinct optimality cuts for the linear approximations of the expected recourse cost and the CVaR of the second-stage. These cutting planes use the retrieved dual solution of the subproblems to delimit the solution space of the master problem. Let ρ_ω^ν be the associated optimal dual solution of the linear program (26) - (28). The coefficients of the eq. (19) and (23) are then calculated as

$$e_i = \sum_{\omega \in \Omega} \pi_\omega \rho_\omega^{\nu\text{T}} h_\omega \quad E_i = \sum_{\omega \in \Omega} \pi_\omega \rho_\omega^{\nu\text{T}} T_\omega \quad (29)$$

$$\hat{e}_{i,\omega} = \rho_\omega^{\nu\text{T}} h_\omega \quad \hat{E}_{i,\omega} = \rho_\omega^{\nu\text{T}} T_\omega. \quad (30)$$

2) *At least one of the subproblems $\omega \in \Omega$ is infeasible:* Such an infeasibility arises when x^{DA^ν} satisfies the first-stage constraints, yet it does not fully consider the implications it lays upon the second stage. In this case we want to generate a cutting plane forbidding the particular solution x^{DA^ν} in the next iteration $\nu + 1$. In order to obtain such a feasibility cut as in (20) we consider a modification of the infeasible subproblem ω

$$Q\left(x^{\text{DA}^\nu}, \omega\right) = \min_{x_\omega^{\text{ID}}, v^-} e^\text{T} v^- \quad (31)$$

$$s.t. W x_\omega^{\text{ID}} - \mathbb{1} v^- \leq h_\omega - T_\omega x^{\text{DA}^\nu} \quad (32)$$

$$x_\omega^{\text{ID}} = \left(P_{t,\omega}^{\text{ID}}, P_{t,\omega}^{\text{Phy}}\right)^\text{T} \quad (33)$$

$$v^- \geq 0. \quad (34)$$

Let ρ_ω^ν again be the associated optimal dual solution for the now modified subproblem ω . We can then determine the coefficients of the feasibility cut (20) as

$$d_j = \rho_\omega^{\nu\text{T}} h_\omega, \quad D_j = \rho_\omega^{\nu\text{T}} T_\omega. \quad (35)$$

After that we continue with the next iteration $\nu = \nu + 1$ and solve the master problem again with the newly added feasibility cut.

If all subproblems have been solved to optimality, the convergence check is performed. As long as the stopping condition is not yet fully satisfied we go back to solving the master problem with the newly added optimality cuts and raise the iteration counter ν by one. In this paper we are using an ε -relaxed stopping condition to abort the iterative decomposition algorithm. We therefore define an absolute tolerance level ε_{abs} . It can be shown that the two introduced optimality cuts are supporting hyperplanes for the expected recourse costs and the CVaR of the second stage. Thus, it follows that at any iteration ν of the algorithm $\theta^{\mathbb{E}^\nu}$ and θ^{CVaR^ν} represent lower bounds to the actual second stage terms

$$\underbrace{\theta^{\mathbb{E}} + \beta \cdot \theta^{\text{CVaR}}}_{=:\theta^\nu} \leq \underbrace{\left(\mathbb{E}\left(Q\left(x^{\text{DA}^\nu}, \omega\right)\right) + \beta \cdot \text{CVaR}\left(Q\left(x^{\text{DA}^\nu}, \omega\right)\right)\right)}_{=:\theta^*}, \quad (36)$$

where the components of θ^* are defined the following way

$$\mathbb{E} \left(Q \left(x^{\text{DA}^\nu}, \omega \right) \right) = \sum_{\omega \in \Omega} \pi_\omega Q \left(x^{\text{DA}^\nu}, \omega \right) \quad (37)$$

$$\text{CVaR} \left(Q \left(x^{\text{DA}^\nu}, \omega \right) \right) = \text{VaR} + \frac{1}{1-\alpha} \sum_{\omega \in \Omega'} \pi_\omega \left(Q \left(x^{\text{DA}^\nu}, \omega \right) - \text{VaR} \right) \quad (38)$$

$$\text{where } \Omega' = \left\{ \omega \mid Q \left(x^{\text{DA}^\nu}, \omega \right) \geq \text{VaR} \right\}.$$

In eq. (38) VaR can be analytically determined by finding the α -quantile of the underlying distribution function for the discrete realizations $Q \left(x^{\text{DA}^\nu}, \omega \right)$ for all $\omega \in \Omega$. Considering the findings in eq. (36) it immediately follows that

$$f^\nu \leq f^*, \quad (39)$$

where f^ν is the optimal objective value of the master problem at a given iteration ν and f^* can be calculated as

$$f^* = f^\nu - \theta^\nu + \theta^*. \quad (40)$$

The stopping condition is eventually given by

$$f^* - f^\nu \leq \varepsilon_{\text{abs}}. \quad (41)$$

Additionally we introduce a stopping condition based on a relative tolerance ε_{rel} and let the algorithm finish as soon as either the absolute or the relative condition is satisfied

$$\frac{f^* - f^\nu}{|f^\nu|} \leq \varepsilon_{\text{rel}}. \quad (42)$$

B. Multicut Benders

The optimality cuts in (19) and (22) aggregate the dual information retrieved by the subproblems by weighting them with their respective probability and thus generating one single cut. In opposition to this so-called singlecut Benders, the dual information can also be used to generate a distinct cutting hyperplane for each of the ID scenarios, accounting for the name multicut Benders. With regard to the nature of the underlying subproblem models it is generally beneficial to consider using the multicut method when the subproblems show a high variance in their stochastic values. In this case singlecut Benders could lead to a too high loss of information on extreme ID scenarios. The above stated singlecut version can be transferred to a multicut version by changing eq. (19) and (22) respectively to

$$\theta_\omega^\mathbb{E} \geq \hat{e}_{i,\omega} - \hat{E}_{i,\omega} x^{\text{DA}}, \quad i = 1, \dots, \tau, \omega \in \Omega \quad (43)$$

$$\theta_\omega^{\text{CVaR}} \geq \text{VaR}_i + \frac{1}{1-\alpha} \eta_{i,\omega}, \quad i = 1, \dots, \tau, \omega \in \Omega. \quad (44)$$

Here, the definition of the coefficients $\hat{e}_{i,\omega}$ and $\hat{E}_{i,\omega}$ does not change compared to eq. (30). Furthermore, $\theta^\mathbb{E}$ will be replaced by $\sum_{\omega \in \Omega} \pi_\omega \theta_\omega^\mathbb{E}$ and θ^{CVaR} by $\sum_{\omega \in \Omega} \pi_\omega \theta_\omega^{\text{CVaR}}$ in the objective function (17) of the master problem.

C. MIP starts and branch-and-bound cut-offs

The master problem represents a computational bottleneck due to the complicating binary decision variables ν_t^{DA} for the unit commitment decisions. This situation is aggravated by the fact that the master problem has to be resolved as soon as new optimality cuts have been added. In order to reduce the computing time, especially for those power plant models that require more Benders iterations, the solver can be provided with a MIP start (mixed integer programming start) for the master problem which serves as an initial and feasible starting point for the black-box branch-and-bound algorithm. Since, as a result of the newly introduced optimality or feasibility cuts, the last obtained master problem solution – in particular the old values for $\theta^{\mathbb{E}}$ and θ^{CVaR} – is no longer feasible for the updated master problem, it can hence not be used as a MIP start. Using the identity in eq. (36) one can nevertheless construct a valid MIP start with the help of the subproblem solutions. Let an optimal solution to the master problem in iteration ν for the two Benders methods (singlecut and multicut) be given by

$$x^{\text{singlecut}^\nu} = \begin{pmatrix} x^{\text{DA}^\nu} \\ \theta^{\mathbb{E}^\nu} \\ \theta^{\text{CVaR}^\nu} \\ VaR_i^\nu, i = 1, \dots, \tau \\ \eta_{i,\omega}^\nu, i = 1, \dots, \tau, \omega \in \Omega \end{pmatrix} \quad x^{\text{multicut}^\nu} = \begin{pmatrix} x^{\text{DA}^\nu} \\ \theta_\omega^{\mathbb{E}^\nu}, \omega \in \Omega \\ \theta_\omega^{\text{CVaR}^\nu}, \omega \in \Omega \\ VaR_i^\nu, i = 1, \dots, \tau \\ \eta_{i,\omega}^\nu, i = 1, \dots, \tau, \omega \in \Omega \end{pmatrix}. \quad (45)$$

Together with the values obtained from eq. (37) and (38) we can then derive a valid MIP start for the next iteration $\nu + 1$

$$x_{\text{MIP start}}^{\text{singlecut}} = \begin{pmatrix} x^{\text{DA}^\nu} \\ \mathbb{E}(Q(x^{\text{DA}^\nu}, \omega)) \\ CVaR(Q(x^{\text{DA}^\nu}, \omega)) \\ VaR_i^\nu, i = 1, \dots, \tau \\ VaR(Q(x^{\text{DA}^\nu}, \omega)) \\ \eta_{i,\omega}^\nu, i = 1, \dots, \tau, \omega \in \Omega \\ \eta_{\tau+1,\omega}, \omega \in \Omega \end{pmatrix} \quad x_{\text{MIP start}}^{\text{multicut}} = \begin{pmatrix} x^{\text{DA}^\nu} \\ Q(x^{\text{DA}^\nu}, \omega), \omega \in \Omega \\ \hat{\theta}_\omega, \omega \in \Omega \\ VaR_i^\nu, i = 1, \dots, \tau \\ VaR(Q(x^{\text{DA}^\nu}, \omega)) \\ \eta_{i,\omega}^\nu, i = 1, \dots, \tau, \omega \in \Omega \\ \eta_{\tau+1,\omega}, \omega \in \Omega \end{pmatrix}, \quad (46)$$

where

$$\eta_{\tau+1,\omega} = \max \left\{ 0, Q(x^{\text{DA}^\nu}, \omega) - VaR(Q(x^{\text{DA}^\nu}, \omega)) \right\} \quad \omega \in \Omega, \quad (47)$$

and

$$\hat{\theta}_\omega = \max \left\{ \max_{i=1,\dots,\tau} \left\{ VaR_i^\nu + \frac{1}{1-\alpha} \eta_{i,\omega}^\nu \right\}, VaR(Q(x^{\text{DA}^\nu}, \omega)) + \frac{1}{1-\alpha} \eta_{\tau+1,\omega} \right\} \quad \omega \in \Omega. \quad (48)$$

Note that the fifth and the seventh vector entry of the generated MIP start – both for the singlecut and the multicut version – are the newly introduced variables in the course of the column generation method of our extended Benders approach. In addition to the MIP start, we can pass the solver a so-called cut-off value. Considering the fact that we try to minimize the master objective function, a cut-off value represents an upper bound to the optimal objective value. The solver can then neglect all nodes in the branch-and-bound tree whose relaxation values are higher than the cut-off value and hence significantly reduce solving time. In our context an upper bound to the optimal value of the overall problem is always given by f^* as defined in eq. (40).

D. Hybridization with closed solution

One of the overall goals of the applied decomposition approach is to achieve a reduction in computing time. However, it was shown that for some instances of our unit commitment problem the extensive, i.e. closed, model formulation performs faster, especially when only considering few ID scenarios. We therefore apply a hybridization concept which exploits the fact that the overall computing time of a model generally correlates with the number of Benders iterations needed. We were able to empirically identify a threshold γ of Benders iterations for which the closed solution outperforms the extended Benders decomposition in terms of solving time. With this knowledge we can implement a hybridization of the two solution concepts without having to test the solving times ex ante. The procedure starts by solving every power plant k for every time slice κ using the extended Benders decomposition at the start of the superordinate Lagrangian iterations. Let $N_{k,\kappa}^{\text{Benders}}$ then be the number of Benders iterations needed for the specific model (k, κ) in a Lagrangian iteration. In case that $N_{k,\kappa}^{\text{Benders}} > \gamma$, the respective power plant model (k, κ) will henceforth be solved as a closed model in all following Lagrangian iterations, but only for the particular time slice κ .

IV. OPTIMIZATION APPROACH OF HYDRO POWER PLANTS

In opposition to the thermal power plants, the hydro power units can be modelled as pure linear programs without binary on/off variables due to their fixed operation costs being almost zero, missing ramp conditions and missing minimum up- and downtimes. The physical power P_t^{Phy} is composed of a turbine part P_t^{Turb} and an additional pump part P_t^{Pump} for pumped storages. For mere annual hydro storages without water pumps, the decision variable P_t^{Pump} is omitted accordingly. Seasonal effects can only be adequately taken into account in the optimization process of storage facilities if the optimization period is extended to the whole simulation period and not cut into time slices as done for the thermal power plants. The initial and end fill levels are given as boundary values to the optimization.

For the solution of the linear storage models, dynamic programming has proven to be considerably more efficient than linear programming, especially in case of yearly simulation periods. The dynamic programming of the hydraulic power plants, however, only allows an isolated consideration of the DA market when calculating the optimal power schedule. In order to also consider the stochastic decisions of the ID stage, the existing solution process is extended by a consecutive second solution stage since a two-stage stochastic linear program over the entire observation period would be disadvantageous with regard to runtime and RAM requirements.

Initially, a mere DA scheduling over the entire simulation period is carried out by applying the dynamic programming approach resulting not only in the specific turbine and pumping schedules, but also in the respective fill levels of the storage reservoirs for the entire simulation period. Subsequently, the fill levels serve as initial and ending fill-level bounds for the second stage including ID decisions, which is optimized in time slices. The hydraulic power plants can thus adapt their schedules to the marketing opportunities on both the DA and the ID market within the framework of the fixed storage limits. Hence, the filling levels of the storage reservoirs remain the same at the cutting edges of the time slices, but can be varied in between. Since the solver provides very efficient solution

TABLE I
COMPARISON OF SOLVING TIMES OF THE DIFFERENT BENDERS METHODS AND EXTENSIONS (MIP STARTS AND CUT-OFFS).

	Without extensions	With extensions	Relative difference
Singlecut	3.477 s	3.006 s	−13.55 %
Multicut	0.945 s	0.503 s	−46.77 %
Relative difference	−72.82 %	−83.27 %	

algorithms for pure linear programs, the hydraulic power plant models can be solved as an extensive closed linear program even with the addition of a stochastic ID stage. An extended Benders decomposition as applied to the thermal power plants can generally be omitted.

V. VALIDATION OF COMPUTATIONAL EFFICIENCY

The model was tested for a benchmark case containing real data for 2014. Thereby, the power plant park within the European interconnected grid/markets was reconstructed considering each individual unit. For this purpose, commercial databases and publicly available data was used [43] [44] [45]. Exogenously fixed (hourly resolved) time series, for the electrical system load, renewables feed-in, other decentralized generators and net transfer capacities were generated using the ENTSO-E-Transparency’s data, as well as market transparency data of EPEX Spot SE [46] [47]. Mustrun time series and available power were derived from published unit schedules. Power plant parameters (gradients, efficiencies, start costs, etc.) were extracted from public studies and expert knowledge [48]. The forecasting errors, i.e. the model’s ID load, were generated from the empirical forecasting errors using of time series analysis methods [49]. If not stated otherwise, the number of ID scenarios wighted with their individual probability of occurence will be 20. With regard to the risk coefficients α (VaR-quantile) and β (risk aversion parameter) we used the values 0.8 and 0.5, respectively. It was however shown that the computational efficiency does not significantly depend on these parameters. The tolerances in the stopping condition where set to $\varepsilon_{\text{abs}} = 10$ and $\varepsilon_{\text{rel}} = 3\%$.

A. Comparison of the different decomposition versions

Initially, we compare the solving time between the singlecut and the multicut version of the extended Benders decomposition as well as the impact of the MIP start and cut-off extensions. Table (I) shows the associated average solving times for all thermal power plant models over the course of the whole simulation year.

It is evident that both with and without the extensions the multicut version of the decomposition yields a significant reduction in runtime. This can directly be linked to the fact that the multicut version generally needs fewer iterations until the stopping condition is satisfied. Figure (1) shows the underlying distribution of required iterations for both the singlecut and the multicut version. Since the vast majority of the models only needs one iteration to fully converge – 94.97 % in the singlecut version and 95.11 % in the multicut version – the abscissa starts at two in

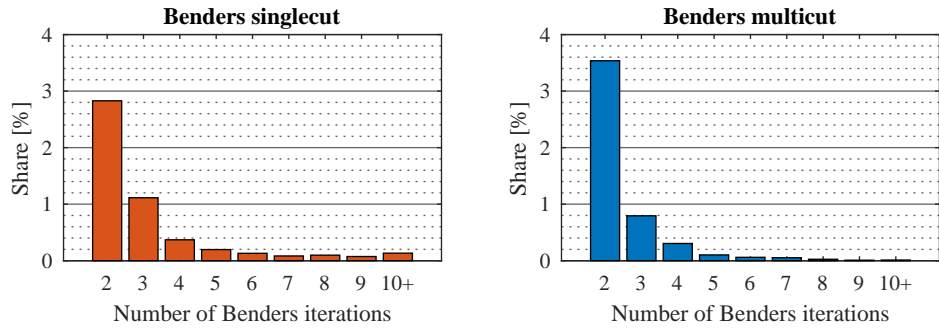


Fig. 1. Distribution of required optimality cuts for all power plant models in case of the singlecut and the multicut version (mind that 94.97% in the singlecut version and 95.11% in the multicut version are solved in one cut).

order to focus on the distribution beyond that value. The share of models that needs more than ten iterations for full convergence is summarized in one bar, accounting for 0.13% in the singlecut version, but only for 0.011% in the multicut version. The global maximum of iterations needed is 22 and 55 for the singlecut and the multicut version, respectively.

Considering the findings so far – especially as far as the reduction of solving time is concerned – we identify the multicut version with the MIP start and cut-off extensions as the most suitable decomposition method for our model instances and henceforth restrict all further examinations and comparisons to this method.

B. Comparison with the closed model solution

Subsequently, we compare the extended decomposition approach with the closed model formulation of the stochastic single unit commitment problem using three criteria: Solving time, RAM requirement and build-up time for the models.

1) *Solving time:* As stated in section III-D we added a hybridization approach to the decomposition method in order to filter those power plant models that can be solved more efficiently in terms of computing time with a closed model formulation. We introduced a break-even-threshold γ which indicates when a plant model should be solved with a closed model instead of the decomposition method in all further superordinate Lagrangian iterations. Figure (2) left shows how γ can be identified empirically. It depicts the average solving times of the decomposition approach for all power plant models as a function of the number of required iterations until full convergence. The abscissa only ranges until seven iterations in order to guarantee a sufficient data basis for the respective values (see figure (1)). In contrast, the figure also shows the corresponding solving times for the same models that have been solved with an extensive closed approach. We can clearly see that the solving time is positively correlated with the number of iterations needed. The hybridization threshold can be identified as $\gamma = 3$.

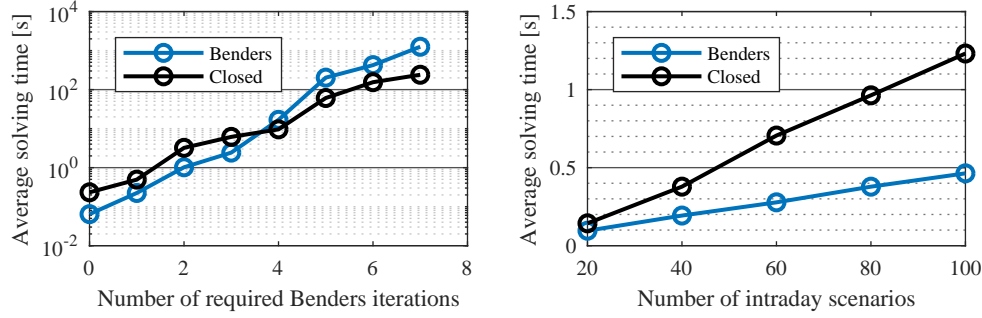


Fig. 2. Average solving time as a function of required Benders iterations and break-even-threshold with closed reference solution (l); Average solving time for an exemplary time slice as a function of considered ID scenarios (r)

TABLE II
COMPARISON OF THE AVERAGE SOLVING TIMES OF THE DECOMPOSITION APPROACH WITH THE CLOSED REFERENCE SOLUTION.

	Closed	Benders	
		Without hybridization	With hybridization
	0.697 s	0.641 s	0.390 s
Solving time benefit	-	8.03 %	44.05 %

Table (II) summarizes the effects on the average solving time of the decomposition approach in comparison to the closed reference solution. The table also reflects the difference in solving time that the applied hybridization accounts for. In the case of the hybridized decomposition approach we see a significant reduction in solving time of about 44 % despite the fact that only a small fraction, namely 1.16 %, of power plant time slice models (k, κ) is being hybridized, i.e. solved as a closed model, in the course of the Lagrangian iterations. The differences of the average solving time of the Benders version without hybridization to the value in table (I) (Benders multicut) can be explained by the fact that we needed to analyze a more progressed Lagrangian iteration in this section in order to guarantee a sufficient saturated level of hybridization.

Figure (2) right concludes the examination of the solving time with a variation of the considered ID scenarios (as stated above only 20 scenarios were used so far). Since we only want to provide an estimation of the growth behaviour of the solving time as a function of ID scenarios, we, for this particular case, have only performed a week simulation on a local machine – instead of a computing cluster, which was used for the yearly simulations. Accordingly, the absolute values of solving time differ from the values found above, but, nevertheless, allow us to come to general conclusions about the runtime growth. For both the closed and the decomposed solution method we can see a linear increase in solving time as a function of considered ID scenarios. In opposition to the closed

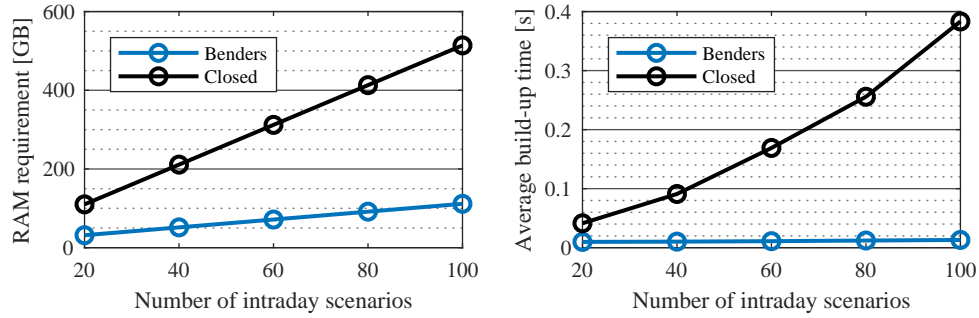


Fig. 3. Overall RAM requirement for storing all models as a function of considered ID scenarios (l); Average build-up time as a function of number of considered ID scenarios (r).

solution, the decomposition approach, however, yields a smaller growth rate amongst a lower offset at already 20 ID scenarios. In conclusion, we can state that the advantageousness of our applied decomposition approach increases with the number of ID scenarios considered.

2) *RAM requirement*: Figure (3) left shows the respective RAM requirement in GB for all thermal power plant models over all time slices as a function of the number of ID scenarios considered. In the case of a closed problem formulation, the memory requirement increases linearly and almost proportionally to the number of scenarios due to the sparse extensive constraints matrix. In contrast, the RAM requirement for the models in the extended Benders formulation is between 71 % and 78 % lower, due to the fact that the model matrices, which are the same for all subproblems, only have to be stored once and account for a dominant share of the total memory requirement. The still observed linear, but this time under-proportional increase of the RAM requirement as a function of ID scenarios can be explained by the memory requirement of the objective function coefficients and the vectors of the right hand side, which are the only ones that differ between the scenarios.

3) *Build-up time*: Since, in the case of our extended decomposition approach, the build-up process of the models – i.e. the composition of the second-stage matrices and other vectors – always consists of the same arithmetic operations, the build-up time required for a given number of scenarios is independent of the concrete model instance, i.e. it is the same for all power plants and all time slices. Figure (3) right depicts the average build-up time as a function of considered ID scenarios for the extended Benders decomposition and the closed solution. While the build-up time increases slightly more than linear with the number of scenarios for the closed problem formulation, it remains constant for the extended Benders decomposition at a significantly lower offset. The largest proportion of time in the build-up process of the closed models is spent on the diagonalization of the extensive second-stage matrices, which takes longer if more scenario matrices have to be diagonalized. This step is omitted in the extended Benders decomposition, which explains the lower and constant setup time.

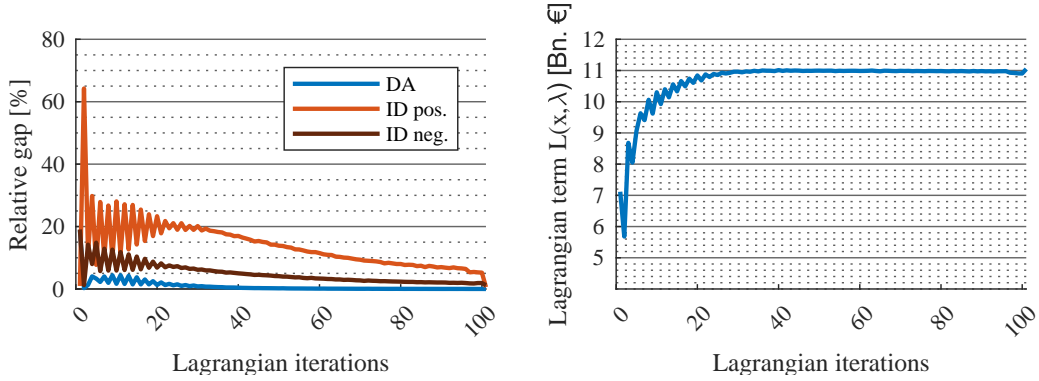


Fig. 4. The convergence process shown through the relative Gaps (l) and the Lagrangian objective (r).

VI. VALIDATION OF CONVERGENCE AND MARKET PRICES

The previous section dealt with the performance of the decomposition used within the single unit optimization. In the following, the performance of the overlaying Lagrangian relaxation is presented and evaluated. The relative gap for the German market area is shown for the relaxed DA constraint as well as for the relaxed (probability weighted) ID constraints – split into both a positive and negative part, since the forecasting errors, in contrast to the positive DA load, may occur in both directions. The gap represents the amount by which the load deviates from the generation in relation to the demanded load (see figure (4) left). Although a dominant opposing zig-zagging between positive and negative ID load coverage amounts can be seen, the procedure eventually converges. The relative gaps on the ID market with 0.6% and 1.2% for the positive and negative forecasting errors, respectively, are higher than the gap on the DA market with exactly 0% (full coverage). The deviations are balanced through a heuristic, which turns on/off power plants, if the resulting unit commitment is insufficient to cover the load. Afterwards, an economic dispatch balances the schedules through a closed linear program (with fixed unit commitment decisions). The objective of the Lagrangian term provides a lower bound for the optimal solution. It should therefore (degressively) increase within the Lagrangian iterations (see figure (4) right converging at around 11 Bn. €). The slight dip in the Lagrangian term in the last iterations arises from the heuristic postprocessing, which cannot guarantee global optimality, but load coverage.

The final Lagrangian multipliers of the relaxed DA and ID load constraint are another important model output as they represent the shadow prices of these constraints. For this model architecture, they therefore represent the DA and ID market prices. Figure (5) shows the simulated German DA and ID prices for the second week of 2014. There is one single DA price for each simulated hour. The ID price is represented by a distribution of prices plotted using statistical quantile analysis. The red cross lines represent the median of the price distribution of the respective hour and the boxes represent the range between the 25% and 75% quantiles. Values beyond this are represented by the dashed vertical lines and the red crosses represent outliers. It can also be seen that volatility in the ID market

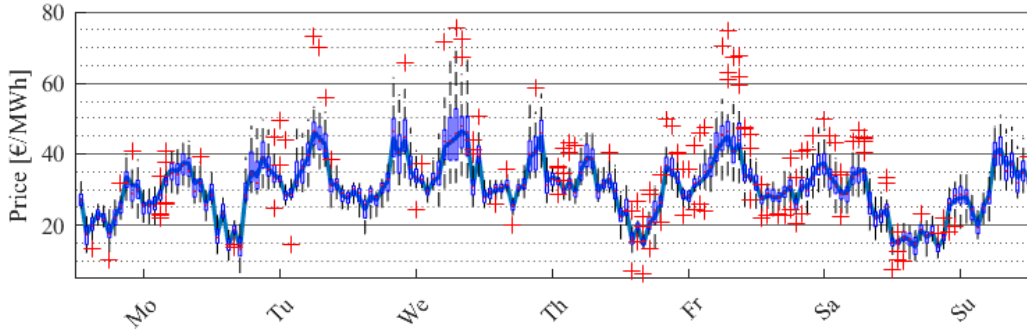


Fig. 5. DA price and ID price distributions (25%-75% quantiles represented by boxes; outliers are red crosses) for the second week of January 2014.

TABLE III
COMPARISON OF EMPIRIC PRICES AND SIMULATED PRICES (MEAN AND STANDARD DEVIATION).

all values in [$\frac{\text{€}}{\text{MWh}}$]	Mean		Std. Dev.	
	DA	ID	DA	ID
Emperical Prices	32.76	33.14	12.77	13.40
Stochastic Optimization	31.37	31.76	7.73	9.14
Deterministic Optimization	31.72	-	7.02	-

is very high, especially in high-price phases. This is due to the fact that in these hours the provision of positive power on the ID market must offer a sufficiently large incentive to refinance turning on additional peak load power plants. The ID price is on average slightly higher than the DA price (see table (III)) - both empirically and in the model. This is due to the fact that the forecasting error has an offset empirically and in the model. However, a risk premium that compensates for price uncertainty on the ID market is endogenously considered. This price offset was also observed in model calculations with no mean value in the forecast errors. The modelled DA price is on average slightly lower than the empirical DA price. In the stochastic model the price is in mean even slightly lower than in the deterministic model. The price spread between DA and ID amounts both in reality and in the model 0.39 €/MWh. The standard deviation of prices in the model is also slightly below real market prices. The stochastic model further results in standard deviations for the DA price slightly above the deterministic model. The standard deviation on the ID market is both empirically and in the model higher than on the DA market.

VII. CONCLUSION AND OUTLOOK

In this paper, a stochastic unit commitment approach taking into account forecasting errors of both REN and electrical load was developed. In contrast to the broad range of classical fundamental electricity market models, which only take into account the unit commitment for the DA market, the ID market to balance forecasting errors

is considered. As a basis for the further development, a European electricity market model based on Lagrangian Relaxation is used [18]. It relaxes the coupling load constraint of each individual market area within the continental synchronous area while endogenously considering market coupling in its subgradient procedure. This allows a systemic decomposition so that the optimization problems of the single units can be solved in an uncoupled manner. This approach has been extended by a set of ID load coverage constraints. Here, the stochastic load in the ID market corresponds to the DA forecasting error. The physical schedule of the power plant and its distribution onto the two markets is thus determined. Due to the immanent price uncertainty in the ID market, the consideration of risk-averse behavior is compulsory in order to depict a more realistic decision behavior. The use of CVaR has proven to be suitable for this purpose. The mixed integer optimization problem grows drastic for each additional ID scenario considered, which leads to a significant increase in computing time if several dozen scenarios are considered. To reduce the complexity when solving optimization problems, a hybrid solution of the closed approach and an L-shaped method with multi-cuts extended by column generation is used. In addition, the master problem was significantly accelerated by using MIP-starts and branch-and-bound cut-offs. In the application to the procedure for the DA and the ID market in Germany, taking into account all DA markets in the European integrated network, a plausible and realistic behavior of the model was shown.

The presented approach provides the basis for systemic analyses with regard to future market developments. Scenarios, such as the TYNDP, the MAF or the eHighway can be used to assess the impact of the ID markets in the future [50] [51] [52]. It can be addressed whether assumptions regarding flexible units from those scenarios, against the background of the increasing dominance of REN, withstand the future supply task from a technical point of view. Furthermore, on the basis of this model, more well-founded evaluations of business cases such as gas power plants, storage facilities, Power2Gas assets, etc. can be carried out. In this model, the electrical load is fixed. However, the increasing penetration of smart homes, which act as prosumers, is steadily increasing. Houses are no longer just rigidly feeding their decentralised photovoltaic feed-in into the grid, but are also optimizing their own consumption using electrical storages and flexible heating systems. The photovoltaic's forecasting error influences the maximization of the individual self-consumption for each of those smart homes. Hence, in a systemic perspective the aggregated residual load of smart homes has an influence on the electrical load. Thus, an influence of the photovoltaic forecasting error on the load forecasting error can be derived, which must be quantified and evaluated. Additionally, the presented decomposition approach is currently not capable of considering integer ID variables, since the dual decision variables of the subproblem, which only exist for linear programs, are necessary in the cut generation. Thus it is not possible to make decisions regarding a unit's start-up (for certain scenarios and only) in the ID market. Due to computational limits the closed approach can not be applied for this case so that further approaches capable of generating cuts in integer subproblems could be integrated [53].

REFERENCES

- [1] Federal Ministry for Economic Affairs and Energy, *Energiekonzept: fuer eine umweltschonende, zuverlaessige und bezahlbare Energieversorgung*, 2010
- [2] General Secretariat of the Council, *European Council (23 and 24 October 2014) - Conclusions*, European Council, 2014
- [3] United Nations, *United Nations Framework Convention on Climate Change - Paris Agreement*, 2016
- [4] United Nations, *Emissions Gap Report 2018*, 2018
- [5] Federal Ministry for Economic Affairs and Energy, *Zeitreihen zur Entwicklung der erneuerbaren Energien in Deutschland unter Verwendung von Daten der Arbeitsgruppe Erneuerbare Energien-Statistik (AGEE-Stat)*, 2018
- [6] International Energy Association, *CO₂ Emissions from Fuel Combustion 2018 - Highlights*, 2018
- [7] A. Conejo, et al., *Decision Making Under Uncertainty in Electricity Markets*, International Series in Operations Research & Management Science, Springer US, 2010
- [8] EPEX Spot SE, *Annual Report 2017* ., 2017
- [9] N. Krzikalla, et al., *Moeglichkeiten zum Ausgleich fluktuierender Einspeisungen aus erneuerbaren Energien*, BET GmbH, 2013
- [10] European Commission, *COMMISSION REGULATION (EU) 2017/2195 of 23 November 2017 establishing a guideline on electricity balancing*, Official Journal of the European Union, 2017
- [11] Poeyry, *NEP2015 - Overview of market model BID3*, 2015
- [12] D. Nailis, et al., *NEMO IV - Gutachten zum Netzentwicklungsplan 2024 im Auftrag der Bundesnetzagentur*, BET GmbH, 2015
- [13] T. Mirbach, *Marktsimulationsverfahren zur Untersuchung der Preisentwicklung im europaeischen Strommarkt*, Dissertation, Aachen, 2009
- [14] H. Stigler, *Gutachten zur Ermittlung des erforderlichen Netzausbaus im deutschen Uebertragungsnetz*, TU Graz, 2012
- [15] H. Natemeyer, et al., *Weiterfuehrende Analysen zur Ermittlung erforderlicher Ausbaumassnahmen des deutschen Uebertragungsnetzes*, RWTH Aachen, 2014
- [16] C. Rehtanz, et al., *Begleitung Netzentwicklungsplan 2025 (NEMO V)*, TU Dortmund, 2016
- [17] C. Rehtanz, et al., *Begleitung Netzentwicklungsplan 2025 (NEMO VI)*, TU Dortmund, 2018
- [18] S. Raths, *Marktsimulationsverfahren fuer einen dezentral gepraeigten Strommarkt*, Dissertation, Aachen, 2019
- [19] T. Drees, *Simulation des europaeischen Binnenmarktes fuer Strom und Regelleistung bei hohem Anteil erneuerbarer Energien*, Dissertation, Aachen, 2016
- [20] C. Chang, et al., *Stochastic: multiobjective generation dispatch of combined heat and power systems*, IEE Proceedings - Generation, Transmission and Distribution, vol. 145, no. 5, 583-591, 1998
- [21] G. Xiong, et al, *Stochastic unit commitment problem considering risk constraints and its improved GA-based solution method*, IEEJ Transactions on Electrical and Electronic Engineering, vol. 8, no. 5, 463-469, 2013
- [22] N. Ramya, et al., *Stochastic Unit Commitment Problem Incorporating Renewable Energy Power*, Swarm, Evolutionary, and Memetic Computing, 686-696, 2015
- [23] F. Bouffard, et al., *Market-clearing with stochastic security*, IEEE Transactions on Power Systems, vol. 20, no. 4, 1818-1826, 2005
- [24] S. Kuhn, *Betriebsoptimierung von elektrischen Energieerzeugungsanlagen und Uebertragungssystemen bei unvollstaendiger Information*, Dissertation, Goettingen, 2008
- [25] Y. Zhang, et al., *Distributed Stochastic Market Clearing with High-Penetration Wind Power*, IEEE Transactions on Power Systems, vol. 31, no. 2, 895-906, 2016
- [26] V. Zavala, et al., *A Stochastic Electricity Market Clearing Formulation with Consistent Pricing Properties*, Operations Research, 2017
- [27] L. Wu, et al., *Stochastic security-constrained unit commitment*, IEEE Transactions on Power Systems, vol. 22, no. 2, 800-811, 2007
- [28] M. Nowak, *Stochastic Lagrangian Relaxation in Power Scheduling of a Hydro-Thermal System under Uncertainty*, Dissertation, Berlin, 2000
- [29] R. Barth, et al., *A stochastic unit-commitment model for the evaluation of the impacts of integration of large amounts of intermittent wind power*, 2006 9th International Conference on Probabilistic Methods Applied to Power Systems, PMAFS, 2006
- [30] D. Swider, et al., *An electricity market model to estimate the marginal value of wind in an adapting system*, 2006 IEEE Power Engineering Society General Meeting, 2006
- [31] A. Tuohy, *Operational and Policy Issues in Carbon Constrained Power Systems*, Dissertation, Dublin, 2009
- [32] F. Abbaspourtorbati, et al., *Three- or Two-Stage Stochastic Market-Clearing Algorithm?*, IEEE Transactions on Power Systems, vol.32, no. 4, 3099-3110, 2017

- [33] H. Brand, *A Stochastic Energy Market Model for Evaluating the Integration of Wind Energy*, 6th IAEE European Conference 2004 on Modelling in Energy Economics and Policy, 2004
- [34] J. Morales, et al., *Electricity market clearing with improved scheduling of stochastic production*, European Journal of Operational Research, vol. 235, 765-774, 2014
- [35] J. Abrell, *Integrating Intermittent Renewable Wind Generation - A Stochastic Multi-Market Electricity Model for the European Electricity Market*, Networks and Spatial Economics, vol. 15, no. 1, 117-147, 2015
- [36] D. Nguyen, *Risk-constrained profit maximization for microgrid aggregators with demand response*, IEEE Transactions on Smart Grid, col. 6, no. 1, 135-146, 2015
- [37] M. Carrion, et al., *A computationally efficient mixed-integer linear formulation for the thermal unit commitment problem*, IEEE Transactions on Power Systems, vol. 21, no. 3, 1371-1378, 2006
- [38] A. J. Wood, et al., *Power Generation, Operation and Control*, Third Edition, Wiley, 2014
- [39] S. Ahmed, *Convexity and decomposition of mean-risk stochastic programs*, Mathematical Programming, vol. 106, no. 3, 433-446, 2006
- [40] R. T. Rockafellar, et al., *Optimization of conditional value-at-risk*, Stochastic Optimization: Algorithms and Applications, Applied Optimization, vol. 54, Springer, 2001
- [41] R.M. Van Slyke and R. Wets, *L-Shaped Linear Programs with Applications to Optimal Control and Stochastic Programming*, SIAM Journal on Applied Mathematics, vol. 17, no. 4, 638-663, 1969
- [42] N. Noyan, *Risk-averse two-stage stochastic programming with an application to disaster management*, Computers & Operations Research, vol. 39, 541-559, 2012
- [43] Platts, *World Electric Power Plants Data Base*, 2016
- [44] German TSO, *Netzentwicklungsplan Strom 2030*, 2019
- [45] RTE., *RTE Open Data platform*, Available: <https://opendata.rte-france.com/>, 2019
- [46] ENTSO-E, *ENTSO-E Transparency Platform*, Available: <https://transparency.entsoe.eu/>, 2019
- [47] EEX, *EEX Market Data*, 2019
- [48] A. Schroeder, et al., *Current and Prospective Costs of Electricity Generation until 2050*, DIW, 2013
- [49] M. Nobis, et al., *Modelling forecasting errors of fluctuating renewables and electrical loads*, 2019 16th International Conference on the European Energy Market (EEM) , 2019 - (Accepted - but not yet published)
- [50] ENTSO-E, *TYNDP 2018 Executive Report*, 2018
- [51] ENTSO-E, *Mid Term Adequacy Forecast 2018*, 2018
- [52] M. Gronau, et al., *D4.3 - Data sets of scenarios and intermediate grid architectures for 2040*, European Commission, 2015
- [53] C. Liu, *Extended Benders Decomposition for Two-Stage SCUC*, IEEE Transactions on Power Systems, vol. 25, no. 2, 2010